Ann. N.Y. Acad. Sci. ISSN 0077-8923

ANNALS OF THE NEW YORK ACADEMY OF SCIENCES
Special Issue: *Countermeasures Against Chemical Threats*

Review

Enhancing organophosphate hydrolase efficacy via protein engineering and immobilization strategies

Priya Katyal,[1,a] Stanley Chu,[1,a] and Jin Kim Montclare[1,2,3,4]

[1]Department of Chemical and Biomolecular Engineering, New York University, Tandon School of Engineering, Brooklyn, New York. [2]Department of Radiology, New York University Langone Health, New York, New York. [3]Department of Biomaterials, New York University College of Dentistry, New York, New York. [4]Department of Chemistry, New York University, New York, New York

Address for correspondence: Dr. Jin Kim Montclare, Department of Chemical and Biomolecular Engineering, New York University, Tandon School of Engineering, 6, Metrotech Center, Brooklyn, NY 11201. montclare@nyu.edu

Organophosphorus compounds (OPs), developed as pesticides and chemical warfare agents, are extremely toxic chemicals that pose a public health risk. Of the different detoxification strategies, organophosphate-hydrolyzing enzymes have attracted much attention, providing a potential route for detoxifying those exposed to OPs. Phosphotriesterase (PTE), also known as organophosphate hydrolase (OPH), is one such enzyme that has been extensively studied as a catalytic bioscavenger. In this review, we will discuss the protein engineering of PTE aimed toward improving the activity and stability of the enzyme. In order to make enzyme utilization in OP detoxification more favorable, enzyme immobilization provides an effective means to increase enzyme activity and stability. Here, we present several such strategies that enhance the storage and operational stability of PTE/OPH.

Keywords: organophosphorus compounds; organophosphate hydrolase; pesticides; chemical warfare agents; phosphotriesterase; organophosphates

Introduction

Organophosphorus compounds (OPs) are classified as neurotoxins since they serve as potent inhibitors of acetylcholinesterase (AChE).[1] OPs are synthetic small molecules first synthesized during the Second World War to serve as insecticides and pesticides; this class of compounds has been further developed as chemical warfare agents (CWAs). OPs have the general structure $O{=}P(OR)_3$, while a subset of compounds have the structure $SP(OR)_3$, $NC\text{-}P(OR)_3$, or $F\text{-}P(OR)_3$ (Fig. 1). Some of the OP-based CWAs include the G-series nerve agents (sarin, tabun, soman, and cyclosarin), V-series nerve agents (VE, VG, VM, VX, and VR), and OP-based pesticides (paraoxon, acephate, diazinon, coumaphos, parathion, chlorpyrifos, and malathion) (Fig. 1 and Table 1).[2,3] Organophosphates contain chiral centers, where the S_P enantiomer is the more toxic version of OP-based CWAs. OPs inhibit the function of AChEs in the human body, which function to break down the neurotransmitter acetylcholine (ACh). The toxic accumulation of ACh can lead to a range of physiological issues, including hyperstimulation, muscle weakness, convulsions, respiratory failure, and even death.[2,4,5] Reversibility of the inhibition reaction is incredibly slow[6] and dependent on the size of the substituent bound to the phosphorus atoms.[7] Generally, the larger the substituent, the slower or more irreversible the process is for AChE to return to its functional state.[7]

OP pesticide self-poisoning is a common form of suicide, according to the World Health Organization; it accounts for one in seven suicides globally.[8,9] Due to its ease of access, paraoxon and other OP pesticides are a significant hazard.[8,9] OP pesticide poisoning can lead to an acute

[a]These authors contributed equally.

doi: 10.1111/nyas.14451

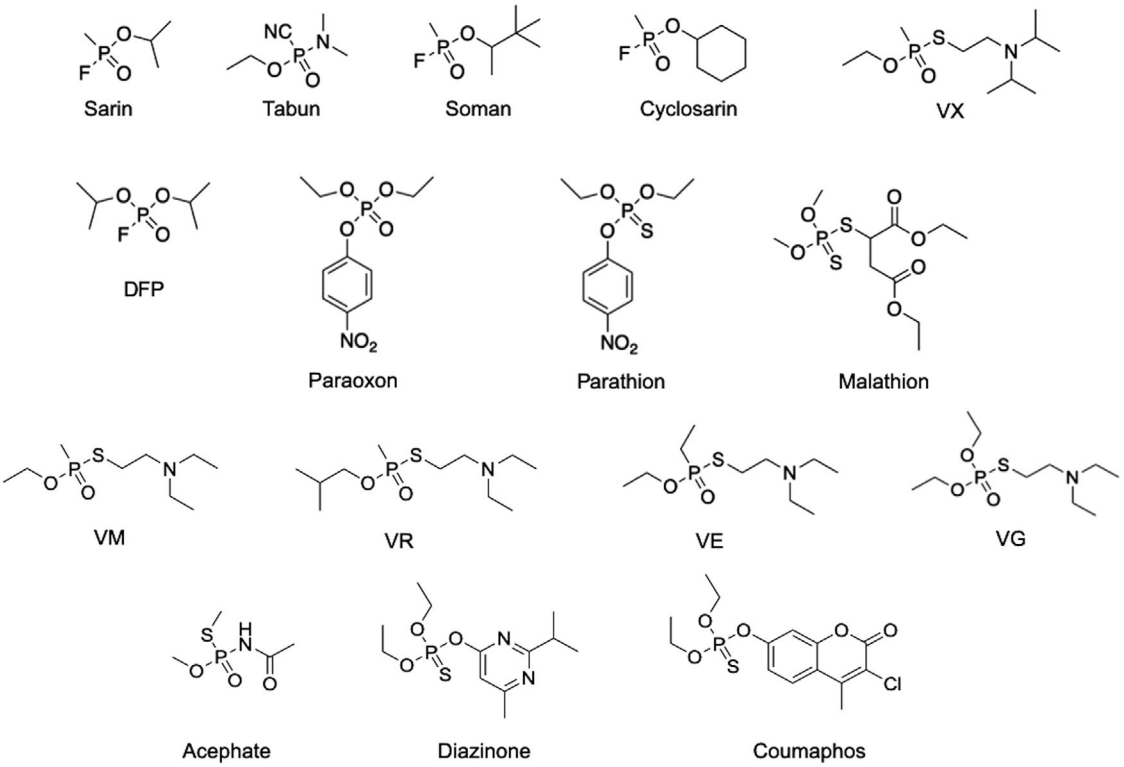

Figure 1. **Chemical structures of OP agents.**

cholinergic syndrome that can be lethal if untreated,[10] as well as several chronic disorders affecting the nervous system,[11] muscles,[12] and heart.[13] Treatment often consists of a cocktail of the muscarinic receptor antagonist atropine for the muscular convulsions, oximes for AChE reactivation, and benzodiazepines for continuing treatment of the nerve agent–induced seizures.[10,14] Therapeutics with antiglutamatergic properties are also being explored to minimize the brain damage associated with prolonged seizure after OP poisoning.[15–18] Treatments have remained relatively ineffective for OP pesticide exposure, with an estimated mortality rate up to 40% for admitted patients.[19]

New technologies are also on the rise for OP poisoning treatment. Nanoparticles (NPs) mimicking red blood cells with AChE on the surface have been shown to decrease the presence of OPs *in vitro* and *in vivo*.[20] An early bioscavenger was butyrylcholinesterase (BChE), capable of binding preferentially to OPs, compared with AChE.[21,22] However, as a stoichiometric scavenger, large amounts of BChE would need to be administered to be effective.[21] The use of an enzyme, particularly wild-type OP-degrading enzyme (OpdA), capable of hydrolyzing G-nerve agents isolated from *Agrobacterium radiobacter*, has shown promise in reducing the OP concentration in African green monkeys.[23] A substantial decrease in dichlorvos, the model OP used in the experiment, after 240 min has been observed without the use of atropine or oximes.

Phosphotriesterase (PTE), an enzyme isolated from *Pseudomonas* species, holds significant promise for OP bioremediation. PTE was first discovered in soil bacterium capable of degrading parathion.[24] Interestingly, PTE has no known natural substrate and broadly degrades a number of synthetically made organophosphates. In particular, PTE seems to have evolved to break down paraoxon at a diffusion-limited rate,[25] indicating that it is optimally evolved to break down paraoxon. Additionally, there is some evidence to suggest that *Pseudomonas* and other microorganisms are able to use OPs as a source of carbon and nutrients.[24] Native PTE has been found to break down a number of OPs and has been the subject of

Table 1. Select G- and V-agents and OP pesticides and their lethal doses

Nerve agent	LD_{50}	References
Tabun (GA)	0.12–0.22 mg/kg	3, 99, 100
Sarin (GB)	41–96 μg/kg	3, 100
Soman (GD)	38–69 μg/kg	3, 100
Cyclosarin (GF)	46 μg/kg	3
Amiton or tetram (VG)	9 mg/kg	101
Edemo (VM)	1.19 mg/kg	102
VX	7–13 μg/kg	3, 100
Russian VX (VR)	11–15.3 μg/kg	3, 100
Paraoxon (POX)	0.32–1 mg/kg	100, 103
Diisopropyl fluorophosphate (DFP)	1.40 mg/kg	100
Parathion	15 mg/kg	101
Coumaphos	15 mg/kg	104
Diazinon	435 mg/kg	101
Malathion	2830 mg/kg	101
Acephate	266–388 mg/kg	105

engineering efforts to improve its performance.[3] PTE was found to protect mice from multiple lethal doses (4–7 × LD_{50}) of paraoxon, diethylfluorophosphate (DFP), and GA.[26] Thus, engineering an improved PTE has significant potential in biomedical, environmental, and homeland defense applications. In this review, we discuss recent developments in the genetic and form factor (i.e., physical and chemical modifications to PTE post-expression) engineering efforts. These efforts aim to improve PTE catalytic efficiency, enzyme stability, and substrate versatility.

Phosphotriesterase

PTE, also known as organophosphate hydrolase (OPH) (EC 3.1.8.1), is an enzyme originally discovered in *Pseudomonas diminuta*, with an identical protein found in *Flavobacterium*,[3] and has a natural ability to degrade OP pesticides, including paraoxon and parathion;[27] however, its activity toward OP CWAs is limited. Wild-type PTE is best suited for the hydrolysis of paraoxon, with its catalytic efficiency approaching the limit of diffusion.[28] Structurally, PTE is a 336 amino acid (36 kDa)[26]–long protein and functionally exists as a dimer (72 kDa)[29] of two TIM barrel subunits (Fig. 2) with a binuclear site for metal ion complexes. Each monomer can complex with two metal ions and the PTE dimer has a total of four metal ions. PTE's natural metal ligand is zinc (Zn^{2+}) but has also been shown to complex with nickel (Ni^{2+}), manganese (Mn^{2+}), cobalt (Co^{2+}), and cadmium (Cd^{2+});[3] however, Zn^{2+} complexes are the most stable, while Co^{2+} complexes are the most active.[29–31] The more solvent-exposed β-metal ion interfaces with the residues His201 and His230 and the other more buried α–ion interfaces with His55, His57, and Asp301.[3,27,32] A carboxylated Lys169 acts as a bridge between the ions.[3] The catalytic site of PTE comprises of a large group pocket (made of residues His254, His257, Leu271, and Met317) and a small group pocket (made of residues Gly60, Ile106, Thr303, and Ser308) (Fig. 2).[3,27,32] Additionally, there is a leaving group pocket made of residues Trp131, Phe132, Phe306, and Tyr309 (Fig. 2).[3,27,32] Protein engineering efforts have been made to give PTE additional promiscuity toward CWAs, enhanced catalytic activity, and improved thermal stability.

Genetic engineering of PTE

Substantial protein engineering efforts have been made to create PTE mutants with improved physical and chemical properties. The catalytic efficiency of wild-type PTE for paraoxon ($k_{cat}/K_M \sim 10^9$ M^{-1} min^{-1})[3,26] approaches the limit of diffusion; however, the catalytic efficiency of PTE for other substrates, notably G- and V-series nerve agents, is several orders of magnitudes lower (k_{cat}/K_M $\sim 10^5$–10^6 M^{-1} min^{-1}).[26] It has been suggested that in order for the enzyme to be used as a biotherapeutic, its efficacy should be on the order of 10^7.[26] Thus, enzyme engineering efforts have been primarily targeted toward increasing the catalytic efficiency of PTE against other substrates, specifically the more toxic S_P enantiomers of nerve agents due to PTE naturally preferring the less toxic R_P enantiomer.[3]

Genetic engineering of the PTE active site

While PTE has the natural ability to hydrolyze a broad range of OPs, it is far too inefficient for therapeutic applications.[33] Thus, enzyme-engineering efforts have been targeted toward improving the catalytic efficiency against nerve agents, specifically the more toxic S_P enantiomer of nerve agents. The crystal structure of PTE has given structural understanding of the critical residues for the catalytic activity of PTE.[34] Thus, substantial genetic

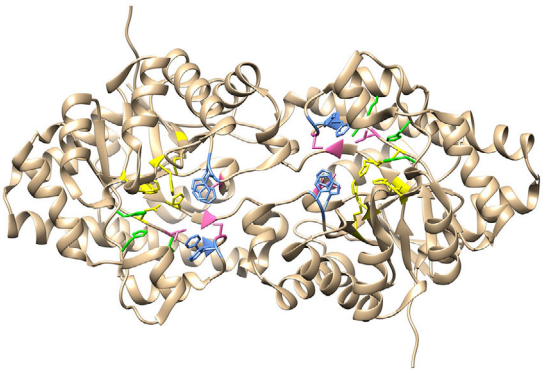

Figure 2. **Cartoon representation of the crystal structure of PTE (PDB ID: 1HZY).[107] The catalytic site is made up of a large group pocket (His254, His257, Leu271, and Met317) in green, a small group pocket (Gly60, Ile106, Thr303, and Ser308) in pink, a leaving group pocket (Trp131, Phe132, Phe306, and Tyr309) in blue, and a metal ligand pocket (His55, His57, Lys169, His201, His230, and Asp301) in yellow.**

engineering efforts have been directed toward the catalytic site of PTE. The Raushel group has identified a general strategy for enhancing the catalytic efficiency toward nerve agents.[35,36] Mutations to enlarge the small binding pocket enhance catalytic efficiency toward nerve agents,[35] potentially through increased steric accommodations for larger substrates.[37] Mutations to reduce the size of the large binding pocket reverse the enantioselectivity to prefer the more toxic isomer.[35,36] A PTE mutant (I106G/H257Y/S308G)[35] prefers the more toxic enantiomer by 460-fold and another variant (H257Y/L303T)[36] demonstrates preference toward the more toxic enantiomers of GB and GD analogs (Table 2). diSioudi *et al.*[37] have also identified an H257L mutant with an 11-fold increase and an H254R/H257L mutant with an 18-fold increase relative to native PTE in specificity toward a GD analog. Interestingly, these mutations cause a decrease in the number of metal ligands from 4 to 2 metal ions per dimer (Fig. 3A and Table 2). Using metal titration and flame atomic absorption spectroscopy, the apoenzyme was found to regain its activity upon titration with two equivalents of cobalt (II) chloride ($CoCl_2$). This loss of metal ions may have introduced additional flexibility to the binding pocket of PTE, conferring improved catalytic efficiency toward VX and GD.

Directed evolution strategies have created large libraries of PTE variants to identify mutants with increased catalytic activity toward nerve agents. The Raushel group[38] has created targeted libraries at two sites in addition to random mutagenesis of the loop regions and identified a PTE variant VRN-VQFL with a 26-fold improvement in activity toward DEVX (Fig. 3B and Table 2), an analog of VX (Fig. 3B, inset). Schofield and Dinovo[4] have performed site-directed mutagenesis of the binding pockets in the catalytic domain of PTE. Their work has identified two PTE variants with 8-fold (mutant 5) and 26-fold (mutant 8) improved activity toward VX (Table 2). Tsai *et al.*[39] have utilized randomized libraries generated by error-prone PCR coupled with site-specific modifications to isolate PTE variants with improved reactivity toward GB, GD, GF, VX, and VR. Specifically, an H257Y/L303T variant was at least 13,000-fold more active toward GB, GD, and GF compared with wild-type PTE (Table 2). Bigley *et al.*[40] have screened a 28,800 mutant library constructed from six-residue saturation mutagenesis and identified several mutants with increases in catalytic efficiency toward CWAs. Notably, one mutant (BHR-23) had a 9200-fold increase in k_{cat}/K_M toward VX compared with wild-type PTE, and another mutant (BHR-73-MNW) had a 13,400-fold increase in k_{cat}/K_M toward VR compared with wild-type PTE (Table 2).

Genetic engineering of PTE outside the catalytic domain

Residues outside the catalytic pocket and metal ligand interface have also proven to be critical in the function of PTE. Studies have demonstrated that diethyl-4-methylbenzylphosphonate (EBP) is a potent competitive inhibitor of wild-type PTE but acts as a noncompetitive inhibitor in some PTE mutants.[41,42] This suggests that the PTE enzyme features an allosteric site that is critical for the activity of PTE. Although this allosteric site has not been extensively studied, this finding illustrates that residues outside the substrate binding pocket and metal ligand interface could be potential candidates for mutation.[42] Indeed, mutations to the PTE surface have yielded mutants with improved catalytic activity. Directed-evolution efforts by Cho *et al.*[43] have been targeted at loop 7, which is on the PTE surface (although near the leaving group binding pocket). These studies resulted in one variant, 22A11 (A14T/A80V, K185R/H257Y/I274N), with a 25-fold improved hydrolysis of methyl parathion

Table 2. PTE mutants and their catalytic efficiencies

PTE mutant	Mutations	Substrate	k_{cat}/K_M ($M^{-1}s^{-1}$)	References
	I106G/H257Y/S308G	Paraoxon derivative	5.1×10^7	35
YT	H257Y/L303T	GB	3×10^5	36, 39
		GD	8.9×10^4	36, 39
		GF	8×10^5	39
	H257L	Paraoxon	5.3×10^7	37
		DFP	2.6×10^4	37
		Demeton-S	1.8×10^3	37
	H254R/H257L	Paraoxon	4.0×10^7	37
		DFP	4.0×10^3	37
		Demeton-S	2.7×10^4	37
VRN-VQFL	A80V/F132V/K185R/H254Q/ H257F/I274N/S308L	DEVX	3.1×10^4	38
Mutant 5	A80V/I106V/F132D/K185R/D208G/ H257W/I274N/R319S	Demeton-S	1.9×10^4	4
		Malathion	4.02×10^4	4
Mutant 8	A80V/I106V/F132D/K185R/D208G/ H257W/I274N/S308L/R319S	Demeton-S	1.99×10^4	4
		Malathion	1.1×10^5	4
BHR-23	F132V/H254R/I274S/S308L	VX	8×10^5	40
BHR-73-MNW	C59M/I106A/F132E//T173N/ H254G/I274N/Y309W	VR	5.8×10^4	40
22A11	A14T/A80V/K185R/H257Y/I274N	Methyl parathion	6.4×10^7	43
		Paraoxon	6.2×10^8	43
B3561	A14T/L17P/A80V/V116I/K185R/ A203T/I274N/P342S	Chlorpyrifos	2.2×10^8	44
G5-C23	F132E/T173N/H254G/P342S	VX	4.99×10^6	51
		VR	3.03×10^6	51
PTE-d1-10-2-C3	K77A/A80M/F132E/T173N/G208D/ D233G/H254G/A270S/L271W/I274N/ Y309W/R118E/A203D/S222D/S238D/ M293V/G348T/T352E	VX	5×10^7	33
d1-IVA1	C59M/K77A/A80V/ I106A/F132E/T173N/G208D/D233G/ H254G/A266D/I274N/Y309W/ R118E/A203D/S222D/S238D/ M293V/G348T/T352E	VR	1.2×10^7	33
Bd-PTE-d2-R2#16	I106H/F132E/L271R/L303T/F306I	GD and GF	$>10^7$	53, 106

(MPT) and up to a 10-fold faster hydrolysis of paraoxon, parathion, and coumaphos (Table 2). Using the 22A11 variant as a parent mutant, they have constructed a library via DNA shuffling and identified an OPH variant, B3561 (A14T/L17P/A80V/V116I/K185R/A203T/I274N/P342S), from two rounds of directed evolution that exhibits a 700-fold hydrolysis improvement for chlorpyrifos (Table 2).[44] Furthermore, Olsen *et al.*[45] have identified residues outside the dimer interface that played critical roles in improving the properties of PTE. Specifically, incorporation of a F306L mutation improves catalytic activity and offers some protection from heat inactivation (Fig. 3C). These experiments show that residues outside the dimer interface and the catalytic domain prove to play an important role in enzymatic performance.

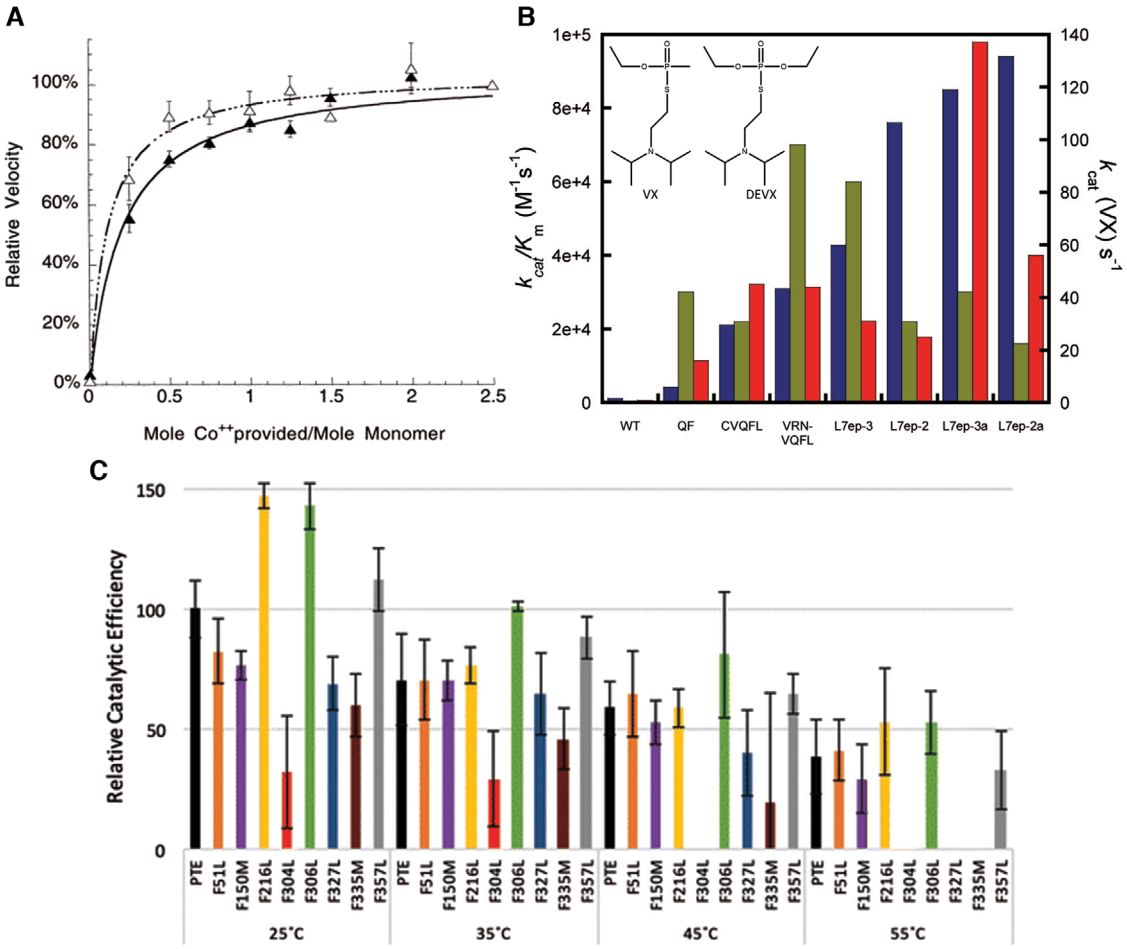

Figure 3. (A) Relative activity against 3 mM paraoxon (closed triangle ▲) and 6 mM demeton-S (open triangle △) of the apoenzyme of the PTE mutant H254R/H257L reconstituted with equivalents of Co^{2+}. The kinetic profile of the PTE mutant begins to plateau at 1 mol of metal per monomer, indicating a loss of 2 moles of metal per dimer. Adapted with permission from diSioudi *et al.*[37] Copyright American Chemical Society. (B) The k_{cat}/K_M values for PTE mutants against DEVX (blue) and VX (green). The red bars indicate the k_{cat} values for the hydrolysis of VX. The mutant VRN-VQFL displayed enhanced catalytic activity against DEVX. The inset shows a comparison of the chemical structure of VX and its analog DEVX. Adapted with permission from Bigley *et al.*[38] Copyright American Chemical Society. (C) Residual activity of PTE mutants with allosteric site mutations at different temperatures. All k_{cat}/K_M values were normalized to PTE at 25 °C. The mutant F306L exhibited improved activity at 25 °C and residual activity after heating to 55 °C compared with PTE. Republished with the permission BioSystems Olsen *et al.*[45]

Improving PTE stability

Native PTE is a fairly stable enzyme, with a conformational stability of 40 kcal/mol.[30] However, engineering efforts dedicated toward improving catalytic efficiencies often come at the cost of enzyme stability, and thus, additional engineering studies have been targeted toward improving the stability of PTE.[30,33] Reeves *et al.*[30] have shown that introducing the mutation H254R/H257F provides 3.88 kcal/mol to the global stability of the enzyme due to electrostatic and van der Waals effects (although it is still less stable compared with the wild-type PTE) (Table 3). The single mutant A80V and variants containing the alteration K185R have beneficial effects in increasing enzyme stability and expression (Table 3).[43] The mutation Y309A was also found to improve expression (Table 3).[46] Introducing additional chemical functionalities, such as disulfide bridges[47] or fluorines,[45,48,49] provides further stability to PTE (see below).

Table 3. PTE mutants for improved stability and their catalytic efficiencies

PTE mutant	Mutations	Substrate	k_{cat}/K_M ($M^{-1}s^{-1}$)	Features	References
RF	H254R/H257F	Paraoxon	9.00×10^6	Stabilized by cation–π interactions	30
		Demeton-S	4.47×10^3		30
2H2	A80V	Methyl parathion	6.0×10^6		43
		Paraoxon	4.1×10^8		43
2H2R	A80V/K185R	Methyl parathion	8.2×10^6		43
		Paraoxon	7.8×10^8		43
	L271A/Y309A	VX	24.9	Wider outer rim of entrance	43, 46
	A204C/T234C	Paraoxon	5.09×10^5	33% retained activity at 65 °C	47
	T128C/E153C	Paraoxon	3.68×10^5	46% retained activity at 65 °C	47
	T199I/T54I	Paraoxon	$k_{cat} = 899.5\ s^{-1}$		50
	C227V/T199I/T54I	Paraoxon	$k_{cat} = 848\ s^{-1}$		50
pFF-F104A	F104A	Paraoxon	2.23×10^6	Global replacement of phenylalanine with fluorophenylalanine	49

Computational design

Recently, computational modeling has proven to be a powerful tool in protein engineering. Although different methods may be used, computational modeling typically performs molecular dynamics simulations to estimate the equilibrium behavior of a protein based on individual amino acid properties. With structural understanding of PTE coupled with sophisticated computational simulation tools, it is possible to perform site mutations *in silico* along with their resulting protein folding energies, thus saving valuable time and resources. The energetically favorable mutations can then be experimentally screened and validated.

Farnoosh *et al.* employed the use of protein simulation software Disulphide by Design and molecular dynamics simulations to identify pairs of residues that would be good candidates for cysteine mutation to enable the formation of disulfide bonds to improve thermal stability.[47] Two mutants, A204C/T234C and T128C/E153C, were identified *in silico* to be good candidates. The T128C/E153C mutant showed increased catalytic activity, while the A204C/T234C mutant showed decreased catalytic activity. Both mutants, however, retained more enzymatic activity at 65 °C compared with the wild type (Table 3). Jacob *et al.* utilized Eris, a molecular modeling simulation that calculates the ΔΔG via side-chain repacking and energy minimization, and identified allosteric mutation sites.[50] These studies generated two variants. Introduction of the double mutation T199I/T54I improved activity up to 70-fold for up to 240 min at 50 °C and up to 30 min at 60 °C (Table 3). The triple mutant C227V/T199I/T54I exhibited improved activity up to 60 min at 50 °C and up to 30 min at 60 °C (Table 3). Jeong *et al.* used docking simulations of VX into the OPH active site to identify key residues to enhance substrate access to the active site.[46] The double mutant L271A/Y309A demonstrated a 150-fold higher catalytic activity for VX compared with wild-type OPH (Table 3). Cherny *et al.* used a combined computational and screen-driven approach to engineer PTE mutants more active toward G- and V-series agents.[51] Rosetta was used to design mutations in the catalytic site docked with a substrate, and a medium-throughput (∼3700 mutants) library was designed via gene reassembly and screened over five rounds (Fig. 4A). A PTE variant (G5-C23) was found that had 5000-fold more activity toward V-agents compared with wild-type PTE (Table 2).

Recent advancements have also allowed for the modeling of noncanonical amino acids (NCAAs). The incorporation of NCAA gives researchers access to more tools in order to create more efficient and stable enzymes. Access to an expanded genetic code offers access to a wider range of chemical diversity. For instance, global replacement of phenylalanine with fluorophenylalanine (pFF) resulted in a variant of PTE (pFF-PTE) that exhibited higher thermal stability and higher catalytic efficiency via the fluorophilic effect (Fig. 4B).[48] Specifically,

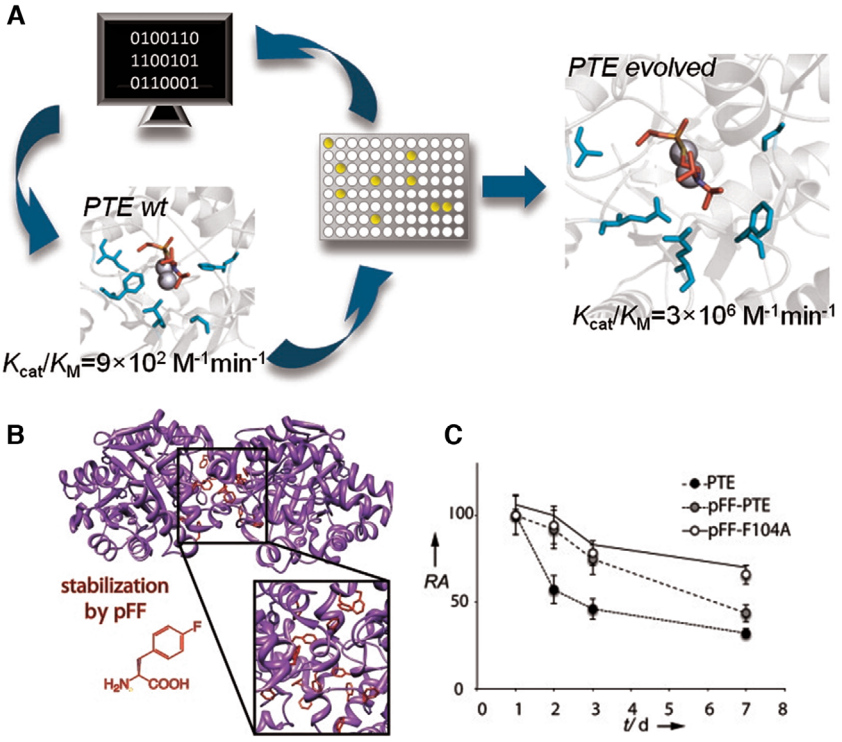

Figure 4. (A) Using Rosetta, VX and VR were docked into the active site of PTE where the best performing variants were tested experimentally. Experimental results were used to refine the Rosetta model in order to identify more variants. In total, five iterations between experimental validation and computational design were performed, resulting in a variant with improved catalytic efficiency. Reprinted with permission from Cherny *et al.*[51] Copyright American Chemical Society. (B) Structural depiction of PTE with phenylalanines replaced by p-fluorophenylalanines at the dimer interface (pFF-PTE). Reprinted with permission from Baker and Montclare.[48] Copyright John Wiley and Sons. (C) Further mutation of F104A (pFF-F104A) improves the residual activity over days. Adapted with permission from Yang *et al.*[49] Copyright John Wiley and Sons.

pFF-PTE exhibited more activity at elevated temperatures compared with wild-type PTE (Table 3). Additionally, fluorination of PTE increased the melting temperature (T_m) by 1–2 °C. However, the introduction of pFF caused steric clashes at the dimer interface as well as solubility issues. Using Rosetta, Yang *et al.*[49] allowed every pFF to freely mutate to other residues except phenylalanine. Using Rosetta, each mutant was allowed to refold and the mutants with the most favorable folding energies were selected. Phenylalanine at position 104 was found to cause steric clashes at the dimer interface, thereby reducing its catalytic activity and stability. This phenylalanine was mutated to alanine to improve stability at the dimer interface (denoted as pFF-F104A). Thus, pFF-F104A demonstrated a higher melting T_m and retained enzymatic activity at elevated temperatures even after several days in solution (Fig. 4C and Table 3). These experiments demonstrate that protein modeling coupled with experimental screening not only generates improved enzyme variants but also expands our understanding of protein dynamics and chemistry.

Challenges in PTE engineering

In order for enzyme scavengers to be used as an effective biotherapeutic for OP decontamination, the catalytic efficiency (k_{cat}/K_M) of engineered PTE should be greater than 10^7 M^{-1} min^{-1}.[33] While engineering efforts have improved the catalytic efficiency of PTE several fold toward other substrates, they still do not reach this threshold. Furthermore, optimization of an enzyme is a nonlinear path[40] and it is difficult to differentiate between local and global optima. For instance, the single mutation of K185R results in the complete loss of PTE activity; however, the double mutation of A80V/K185R improves

enzyme stability and expression and results in a two-fold increase in k_{cat}/K_M against MPT (Table 3).[43] Improvement of PTE also comes with diminishing returns, with every mutation making it increasingly difficult to engineer PTE variants with high catalytic efficiencies (10^7 M^{-1} min^{-1}).[30]

Engineering broad substrate specificity often comes at opportunity costs as well. While some studies have reported some improved PTE variants that do not compromise catalytic activity toward other substrates,[44] the majority of studies report that there is a tradeoff in substrate specificity during engineering efforts.[33,37,41,48,52] To overcome this, the Tawfik group has recently introduced a cocktail of three engineered PTE variants, with each of the three designed to effectively hydrolyze G- and V-series nerve agents. The cocktail is composed of PTE-d1-10-2-C3[33] ($k_{cat}/K_M = 5 \times 10^7$ M^{-1} min^{-1} toward VX), d1-IVA1[33] ($k_{cat}/K_M > 10^7$ M^{-1} min^{-1} toward VR), and Bd-PTE-d2-R2#16[53] ($k_{cat}/K_M >$ 10^7 M^{-1} min^{-1} toward GD and GF) (Table 2). The mixture of the three variants does not show cross-interference in catalytic activity. The mixture also exhibits thermostability above 60 °C and resistance to acidic pH (pH 5–6).

Stabilization/immobilization strategies

Enzymes are fragile molecules that are highly effective under specific conditions. External stresses, such as high temperature, extreme pH conditions, and organic solvents, can denature enzymes or disrupt their active conformation, ultimately compromising their catalytic activity.[54] While protein engineering is an established method to generate libraries of variants with improved catalytic efficiency and stability, exposure or transportation of these enzymes under nonideal conditions can render them useless. Several strategies have been explored that can stabilize OPH. Here, we summarize such strategies (Table 4) that can dramatically increase OPH/PTE performance and confer long-term storage stability.

The most common strategy to stabilize proteins is the use of excipients. Additives, such as sugars, polyols, detergents, polymers, and amino acids, can minimize protein aggregation and influence protein stability.[55] Iyengar *et al.* have screened a panel of excipients that can stabilize OPH (derived from *Flavanobacterium)* under aqueous and lyophilized conditions at 25 °C.[56] Of all the excipients, maltose, trehalose, proline, and arginine were the most effective stabilizers of OPH when stored under aqueous conditions. While freeze-drying of OPH decreased its activity by 20%, addition of sugars (maltose, trehalose, and mannose) during lyophilization preserved its paraoxon-hydrolyzing abilities and improved its stability for 2 months at 25 °C (Table 4).[56]

Another notable example of a sugar that can aid in enzyme solubilization and immobilization is beta-cyclodextrin (CD), a cyclic oligosaccharide consisting of a hydrophobic cavity and a hydrophilic surface.[57] The ability of CD to form host–guest complexes has garnered considerable interest, especially for industrial applications and environmental protection. Owing to its sorption capacity, CD can absorb and detoxify various OPs, including malathion, sarin, and soman.[58] When OPH is immobilized onto poly-cyclodextrin (PCD), CD molecules not only adsorb OPs but also enhance its functional stability and activity (Fig. 5A and Table 4). CD-coated OPH can hydrolyze methyl paraoxon (MPO) within 10 min of exposure and can be reused for a total of four cycles.[59]

Apart from sugars, polymers can also influence the activity and stability of OPHs. Specifically, chemical modification of proteins using polyethylene glycols (PEGs), also referred to as PEGylation, can substantially alter the physicochemical properties of the enzymes. PEGylated proteins exhibit low immunogenicity, high stability, improved pharmacokinetic profiles, and delayed plasma clearance.[60] These features impart pharmacological advantages to the enzymes, enhancing their therapeutic and prophylactic use in managing OP-related toxic effects. Covalent conjugation of OPH with *N*-hydroxysuccinimide (NHS) esters of linear and branched PEG (Fig. 5B and Table 4) adversely impacts the k_{cat} values, reducing the catalytic activity in hydrolyzing paraoxon and demeton-S.[61] In spite of its reduced activity, PEGylating OPH improves its biological efficiency. Both linear and branched PEG improve the circulation half-life of OPH in guinea pigs, with branched PEG exhibiting the maximal effect with enhanced pharmacokinetic profile and lower immunogenicity.[61] Although PEGylation reduces catalytic activity, it can enhance enzyme stability, with OPH still

Table 4. Immobilization strategies of OPH

Stabilization strategy	Pesticide used	Feature(s)	References
Additives	Paraoxon	Stable for 2 months at 25 °C	56
Cyclodextrin	Methyl paraoxon	Recycled for 4–5 times Continuous degradation for 4 days	59
Linear and branched PEG	Paraoxon Demeton-S	Enhanced pharmacokinetic profile and lower immunogenicity in guinea pigs	61
PEG-CA photostabilized gel	Paraoxon	Stable for 7 days at 25 °C	62
Poly(carboxybetaine) (PCB)	Paraoxon Sarin	Stable for 6 months at 4 °C Protective effect of a single prophylactic injection in Sprague–Dawley rats	63
Pluronic blend	Paraoxon	Active in methanol Stable at high temperatures Withstand lyophilization	64
Crosslinked enzyme-Pluronic conjugates (CLEPCs)	Malathion	Enhanced activity in anionic, nonionic, and biocompatible detergents	65
Pluronic micelles (OPH with corona)	Paraoxon	Stable at high temperature, organic solvents, and can withstand lyophilization and multiple freeze–thaw cycles Capable of decontaminating CARC surfaces	66
POEGMA-*b*-qP4VP-Inverse micelles	Methyl paraoxon	Active in ethanol	68
POEGMA-*b*-qP4VP-PAA coacervates	Methyl paraoxon	Improved stability in ethanol and DMMP Active for 3 days after heat treatment at 37 °C	68
Polyelectrolyte multilayers	Methyl parathion	Active under high-salt conditions	69
RHP-PEO fiber mats	Methyl parathion	Seven-fold active in toluene Trap catalytic byproducts	71
Polyurethane foams	Paraoxon	Stable over a 3 months period at RT Resistant to proteases for 125 days at 30 °C	73, 74
Silk fibroin	Methyl parathion	Stable at high temperature, upon UV light exposure, and in the presence of detergents	77
Amyloid fibrils	Paraoxon	Stable at 40, 45, and 50 °C	78
Gelatin pads	Methyl parathion Sarin	Stable for 6 months at RT or a year at 4 °C	79
Resealed carrier erythrocytes	Paraoxon	Stable for 2 weeks at 4 °C	80
Sterically stabilized liposomes (SLs)	Paraoxon	Enhanced protection of OPH Stable in buffer and guinea pig plasma for 4 days	82
DPPC-DVBA	Methyl parathion	Can be lyophilized Stable at room temperature for 3 weeks	83
Magnetic nanoparticles	Ethyl parathion	Stable at extreme pH Can be recycled seven times	86
Graphene oxide	Methyl parathion	Stable in methanol and DMSO Can be stored for 30 days at 4 °C Can be recycled 10 times	87
Mesoporous silica	Paraoxon	Improved immobilization efficiency and stability	88, 89
Nylon powder 11	Paraoxon	Stable for at least 20 months at 5 °C	90
Nylon 6 and 66 membranes	Paraoxon, ethyl parathion, and DFP	Limited activity in hydrolyzing OPs and CWA in the presence of cosolvent	90
OMV	Paraoxon	Stable at high temperature Can withstand lyophilization and multiple freeze–thaw cycles	98

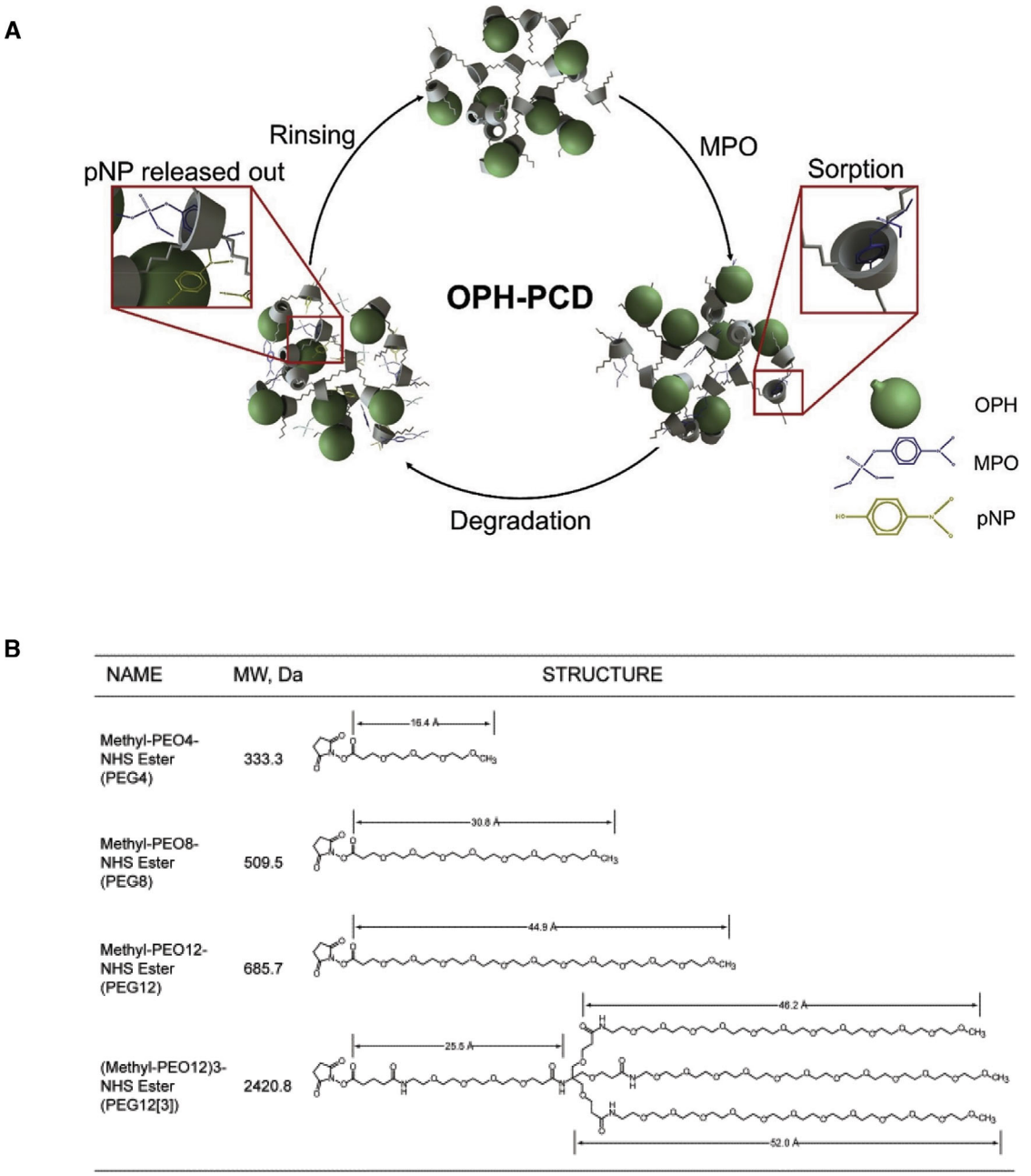

Figure 5. (A) Schematic showing OPH-PCD capable of sorption and degradation of MPO. OPH degrades MPO into para-nitrophenol (pNP) and phosphonic acid. Reprinted (adapted) with permission from Moon *et al.*[59] Copyright Elsevier. (B) Molecular structures of linear and branched polymers. Reprinted (adapted) with permission from Novikov *et al.*[61] Copyright Elsevier.

maintaining substantial activity in OP hydrolysis.[62] Upon exposure to >300 nm light, a mixture of cinnamaylidene-terminated PEG (PEG-CA) and OPH conjugated to PEG-CA can undergo photogelation in the presence of erythrosin B (Table 4). The photostabilized PEGylated OPH within the gel can maintain 80% of its activity over a period of 7 days at 25 °C.[62] OPH can also be encapsulated within a zwitterionic polymeric gel comprising poly(carboxybetaine) (PCB).[63] Unlike PEG,

coating with PCB has no adverse effect on catalytic efficiency of OPH against paraoxon. The polymeric gel significantly improves the storage stability with OPH being active for 6 months at 4 °C under aqueous conditions. In Sprague–Dawley rats, OPH-PCB gel (also referred as nanoscavenger) exhibits prolonged half-life and minimal immune response (Table 4). A single prophylactic injection of these nanoscavengers can protect rats from paraoxon poisoning for a period of 7 days. The nanoscavengers are also effective against G-type nerve agents. A prophylactic injection of PCB gels encapsulating a variant of OPH, referred to as OPH-YT, can protect guinea pigs from toxic effects, even after multiple exposures of sarin (Table 4).[63]

Pluronic, a triblock polymer comprising of poly(ethylene oxide-*b*-propylene oxide-*b*-ethylene oxide) (PEO–PPO–PEO), is another polymer that is quite often used to stabilize OPH. A simple blend of OPH with F127 Pluronic can significantly improve OPH activity against paraoxon (Table 4).[64] A 1:1000 mixture of OPH:Pluronic can maintain its activity in methanol, a solvent commonly utilized to dissolve OPs. Interaction of OPH with the hydrophobic PPO block protects the enzyme from aggregation. Even after heating the mixture at 70 °C for 10 min, the enzyme retained 85% of its activity. The mixture can also be lyophilized and stored for 25 days at 4 °C without significant loss in activity.[64] Besides Pluronic–OPH blends, crosslinked enzyme aggregates (CLEAs) and crosslinked enzyme–Pluronic conjugates (CLEPCs) have also been prepared and tested for OPH activity against malathion (Table 4).[65] Cheng *et al.* have utilized glutaraldehyde to crosslink ammonium sulfate–precipitated OPH in the presence and absence of Pluronic to form CLEPC and CLEA, respectively.[65] CLEPC exhibits better activity and stability with respect to different pHs and temperatures. The crosslinked polymeric conjugates also show improved activity in the presence of detergents, including sodium dodecyl sulfate (anionic), alkyl polyglycoside (nonionic), and coconut oil derivatives (biocompatible detergents).[65]

F127-Pluronic, being an amphiphilic polymer, can assemble into micelles above its critical micelle concentration (CMC).[66] Similar to the NHS ester of PEG (see above), F127-NHS can conjugate with the lysine residues of OPH (Fig. 6A). When used above its CMC, the PPO hydrophobic block of F127 forms the core, while the hydrophilic PEO block, conjugated to OPH forms the corona of the micelles. The micelles, about 100 nm in size, exhibit higher enzymatic activity against paraoxon compared with unconjugated OPH. Conjugated OPH micelles are stable under a variety of conditions, including high temperature and organic solvents, and can withstand lyophilization and multiple freeze–thaw cycles (Table 4). Suthiwangcharoen and Nagarajan have demonstrated the efficacy of these conjugated micelles in decontaminating chemical agent–resistant coating (CARC) surfaces (Fig. 6B).[66]

OPHs are also stable as reverse micelles, where the enzymes are entrapped within the aqueous core surrounded by hydrocarbon tails.[67] Since the enzyme molecules are sequestered within the core, enzymes are protected from the deleterious effects of organic solvents. A block polymer of poly(oligo(ethyleneglycol) methacrylate)-*b*-poly(4-vinyl *N*-methylpyridyl iodide), (POEGMA-*b*-qP4VP), which forms inverse micelles, can enhance OPH activity against MPO for several days (Table 4).[68] These micelles retain 37 $\pm$ 2% (relative to OPH in solution) of OPH activity in ethanol. When POEGMA-*b*-qP4VP is mixed with an oppositely charged polymer, poly(acrylic acid) (PAA), complex coacervate core micelles (C3M) are formed as a result of phase separation. OPH with C3Ms is condensed within the dense polymeric-rich phase that can stabilize enzymes in organic solvents, with OPH exhibiting improved stability in ethanol and dimethyl methyl-phosphonate (DMMP). The OPH-bearing C3Ms also retain its activity for 3 days after heat treatment at 37 °C (Table 4).[68]

Sustained activity of OPH against MPT, extending to about 6 months at room temperature (RT), has been demonstrated by Lee *et al.*[69] OPH immobilized within polyelectrolyte multilayers (PEM) of branched polyethylenimine-polystyrene sulfonate (BPEI-$(PSS\text{-}BPEI)_3$) is deposited onto glass beads via a layer-by-layer approach.[69] The multilayer assemblies are further stabilized by coating the enzyme layer with PEI-PAA and the end-capping monomers 1,2-dihydroxypropyl methacrylate (DHPM), 1,2-dihydroxypropyl 4-vinylbenzyl ether (DHPVB), and *N*-[3-(trimethoxysilyl)propyl]ethylenediamine (TMSED), which are readily polymerized by ultraviolet (UV) light.

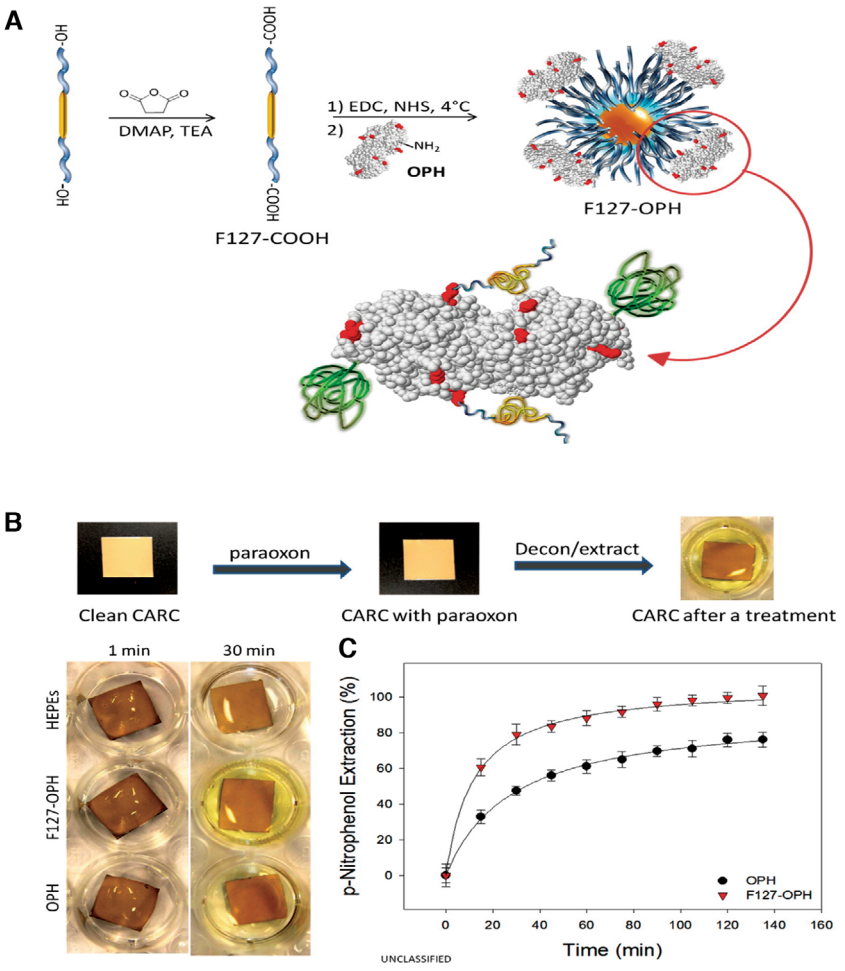

Figure 6. **(A) Conjugation of OPH with F127 Pluronic to form micelles with an OPH corona. (B) Decontamination of CARC using F127-OPH micelles. (C) Enzymatic activity of OPH versus F127-OPH micelles. Reprinted (adapted) with permission from Suthiwangcharoen and Nagarajan.[66] Copyright American Chemical Society.**

The polymer-encased multilayer assembly, in particular, the assembly with crosslinked TMSED, can protect the enzyme from deactivation and delamination under high-salt conditions. OPH stabilized with TMSED coating retains 27% of the original activity under high-salt conditions of 2 M sodium chloride (Table 4).[69] PEM-based coatings are also utilized in designing smart clothing.[70] OPH stabilized within BPEI multilayers maintains MPT-hydrolyzing activity when coated on fiberglass or cotton threads, unveiling new opportunities in designing materials with self-decontamination properties.[70]

The use of polymer-based fiber mats to solubilize and stabilize OPH is another effective approach in OP bioremediation.[71] Panganiban *et al.* have developed a random heteropolymer (RHP) comprising methyl methacrylate (MMA), oligo(ethylene glycol) methacrylate (OEGMA), 2-ethylhexyl methacrylate (2-EHMA), and 3-sulfopropyl methacrylate potassium salt (3-SPMA) at a ratio of 5:2.5:2:0.5.[71] RHP facilitates OPH solubilization in organic solvents, increasing the overall activity of OPH by seven-fold against MPT dissolved in toluene (Table 4). RHP-OPH immobilized on electrospun polyethylene oxide (PEO) or poly(methyl methacrylate) fiber mats was effective in degrading MPT, with PEO-based fiber mats capable of trapping the hydrolysis byproducts (Table 4). These mats allow easy removal of OP

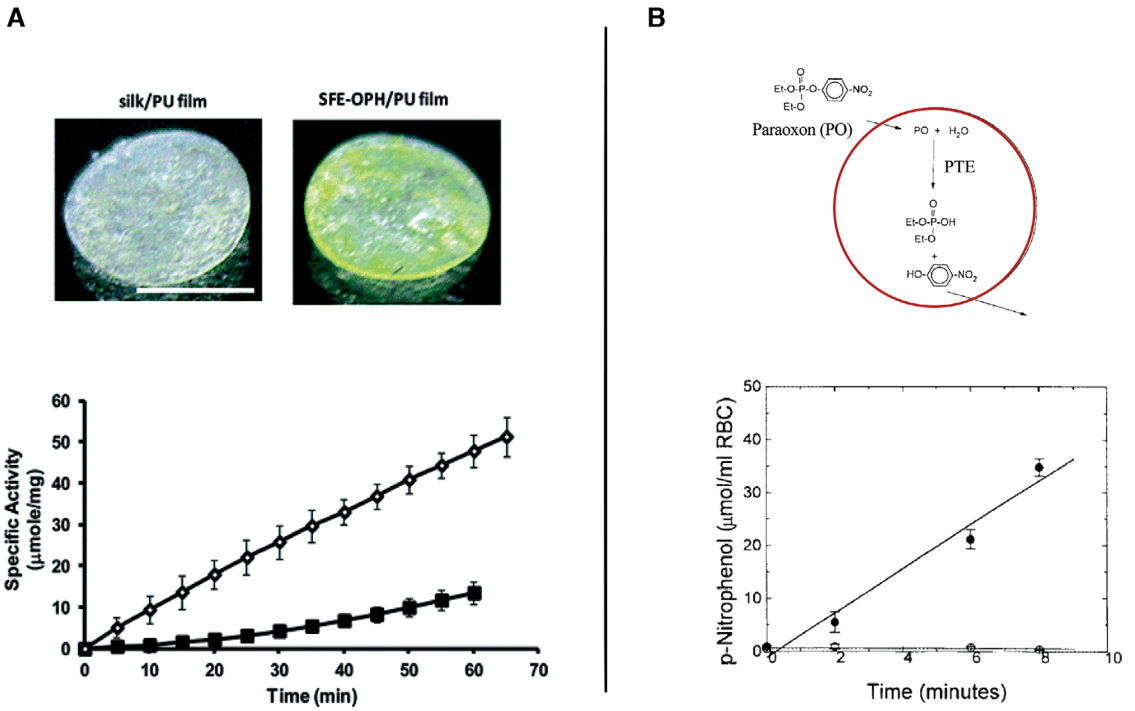

Figure 7. (A) Polyurethane films containing silk fibroin and SFE-OPH placed in MPT solution. The films were incubated at 37 °C for 1 hour. The SFE-OPH/PU film turned yellow due to p-nitrophenol, a hydrolytic product of MPT. The graph shows the hydrolytic activity of SFE-OPH/PU films (open diamond) and PU films containing free OPH (filled squares). Adapted with permission from Dennis *et al.*[77] Copyright American Chemical Society. (B) PTE entrapped within murine erythrocytes is capable of hydrolyzing paraoxon (PO). The graph shows hydrolysis of PO by erythrocytes with respect to time, with PTE (filled circle) and without PTE (open circle). Adapted with permission from Pei *et al.*[80] Copyright Elsevier.

and its byproducts, providing a facile approach to perform on-demand bioremediation.[71]

Alternatively, PTE has been immobilized on polyurethane foams and sponges that can be utilized to clean up small spills.[72–74] Isocyanate-functionalized polyurethanes react with water to form carbamic acid that results in the formation of primary amines and carbon dioxide. While carbon dioxide forms the sponge-like matrix, primary amines can react with isocyanate groups to form urea linkages. The enzyme is then immobilized within the crosslinked isocyanate-functionalized polyurethanes. The foams are active against paraoxon for over 3 months at RT and are resistant to proteases for 125 days at 30 °C (Table 4).[73,74] To decontaminate large areas exposed to OPs, a unique approach of incorporating OPH in firefighting foams has been reported by LeJeune *et al.* Although OPH experiences some loss in its activity, it maintained 30% of activity, capable of neutralizing OP-contaminated surfaces.[75]

Silk fibroin is a unique biopolymer that is increasingly being used for encapsulation of enzymes, antibodies, and biological samples.[76,77] It is a fibrous protein obtained from the cocoons of *Bombyx mori* that exerts a stabilizing effect on encapsulated enzymes, even without the need for chemical crosslinkers.[77] Dennis *et al.* have encapsulated organophosphorus hydrolase in silk fibroin films and tested for its stability and activity against MPT.[77] While hydrated OPH-encapsulated silk fibroin films (SFE-OPH) maintain 70% of original activity for 65 days, dry films retain 60% of its activity for 17 weeks when stored at RT.[77] The films preserve OPH activity under a variety of conditions, including high temperature, UV light, and the presence of organic solvents and detergents (Table 4). Polyurethane films containing lyophilized SFE-OPH powder (Fig. 7A) exhibit higher stability under extreme conditions.[77] Amyloid fibrils, obtained from bovine insulin, are another protein scaffold that has been employed to

immobilize OPH. Fibrils crosslinked with OPH via glutaraldehyde significantly improve thermal stability at 40, 45, and 50 °C (Table 4).[78]

Gelatin pads, which exhibit improved storage stability, have also been utilized to immobilize OPH.[79] Owing to its biocompatibility, the pads can be placed over OP-contaminated skin and surfaces. Homogenized gelatin (gelatin foams) are lyophilized to form pads that are then soaked in glutaraldehyde solution followed by a subsequent soak in OPH. Glutaraldehyde allows covalent crosslinking of OPH with gelatin. These pads are effective in hydrolyzing MPT and sarin even after long-term storage of 6 months at RT or a year at 4 °C (Table 4).[79]

Another interesting approach to protect OPH enzymes is to utilize resealed carrier erythrocytes (Fig. 7B).[80] Pei *et al.* have employed murine erythrocytes to encapsulate PTE. A hypotonic buffer solution is used to create transient pores in the cell membrane, which allows PTE to diffuse through. Once PTE is encapsulated, the cells are resealed using an isotonic solution. A 30% encapsulation efficiency was observed for PTE that remained stable for 2 weeks at 4 °C (Table 4). Encapsulated PTE can rapidly breakdown paraoxon, as compared with free red blood cells.[80] Compared with resealed erythrocytes, sterically stabilized liposomes (SLs) exhibit better encapsulation efficiency (80%) of PTE and have longer storage stability in buffer and plasma.[81,82] The OPH-loaded SLs, comprising palmitoyloleoylphosphocholine (POPC), dipalmitoyl-phosphatidyl phosphoethanolamine-*N*-[(polyethylene glycol)-2000] (PEG-PE-2000), and cholesterol (CHOL), are effective in hydrolyzing paraoxon (Table 4). These liposomes are capable of protecting mice against the toxic effects of OPs and exhibit enhanced protection compared with atropine and 2-PAM.[82] Other examples of OPH-loaded lipid-based vesicles include dipalmitoyl-sn-glycero-3-phosphocholine (DPPC)–based lipid nanocapsules, as reported by the Singh group.[83,84] These nanocapsules consist of 3,5 divinylbenzoyl (DVB) headgroups, which can undergo photopolymerization and crosslinking at 254 nanometers. The crosslinked nanocapsules can be freeze-dried and retain 18% of original activity against MPT when stored at RT for 3 weeks (Table 4).[83]

Of the several stabilizing strategies, enzymes immobilized onto magnetic iron NPs can be readily separated by external magnetic fields.[85] Enzyme immobilization onto these NPs makes them both catalytically effective and recyclable. Robatjazi *et al.* have covalently attached OPH to amino-functionalized magnetic NPs via *N*-ethyl carbodiimide.[86] These NPs are stable under extreme pH conditions and exhibit a 6.3-fold improvement in enzyme activity against ethyl parathion for 5 days at 4 °C (Table 4). The magnetic particles can easily be used and recycled for seven times, with 73% of enzyme activity retained even after the seventh cycle, indicating their potential in bioremediation and biosensing.[86] Graphene oxide (GO) is another bioinorganic matrix that is employed to immobilize OPH.[87] Nanocapsules of acryloylated OPH immobilized on GO, referred as nOPH10@GO, exhibit improved activity, stability, and reusability (Table 4). nOPH10@GO is stable in methanol and DMSO and can be stored for 30 days at 4 °C. Interestingly, the polymer-stabilized OPH on GO maintains 90% of original activity, even after 10 successive cycles of reuse.[87] Aside from the abovementioned bioinorganic matrices, organically functionalized mesoporous silica (FMS) has been effectively utilized to encapsulate OPH. HOOC-FMS, bearing (-CH_2-CH_2-COOH), showed exceptional immobilization efficiency and stability after long-term storage for 145 days.[88] Amine-functionalized crosslinked mesoporous silica particles reported by Frančič *et al.* also exhibit high immobilization efficiency, capable of hydrolyzing paraoxon for up to eight cycles.[89]

Long-term stabilization of PTE has also been reported when PTE is immobilized onto nylon powder.[90] PTE crosslinked with glutaraldehyde-treated nylon powder 11 (mesh size 140) was shown to be stable for 20 months at 5 °C. The large surface area of the powder particles allows sorption of highly concentrated enzymes, achieving faster hydrolysis of paraoxon. Apart from nylon powder, nylon membranes have also been utilized to immobilize PTE.[90] Compared with nylon powder, immobilization of PTE onto nylon 6 and nylon 66 membranes significantly affects its catalytic efficiency. Despite having a higher Km in the presence of a cosolvent, immobilized PTE, in particular with nylon 66 membrane, limits its activity to 10% of free enzyme. Even with such reduced activities, immobilized PTE has been shown to hydrolyze dilute solutions of paraoxon

or ethyl parathion and attain partial hydrolysis of DFP.[90]

Several other substrates, including cellulose microfibers,[91] chitosan beads,[92] quantum dots,[93] carbon nanotubes,[94] gold NPs,[95] and agarose beds,[90] have been utilized to immobilize OPH. Some of these substrates are best suited for fabricating novel biosensors for OP detection and are discussed elsewhere.[2,96] The immobilization strategies described in this article hold promise as therapeutics and as agents for environmental decontamination. Each strategy has its special use, and the choice of specific immobilization method is influenced by the overall cost, scalability, and applicability. Over the past few years, significant interest has been generated in developing systems that combine one or more strategies.[97,98] For example, Alves *et al.* have utilized bacterial outer membrane vesicles (OMVs) to package PTE enzyme. These OMVs, referred as proteoliposomes, combine proteins, lipids, and polysaccharide components, exerting a synergistic effect on PTE activity and long-term storage stability (Table 4).[98] Although these vesicles show promise, they have yet to be tested in real-world applications.

Conclusions

OP-based pesticides and CWAs pose a great risk to civilians and military populations. Enzyme-based approaches, in particular, OPH/PTE enzymes, have offered a potential route of OP detoxification. Extensive research has been devoted to generating stable and active variants of OPH/PTE that exhibit improved efficacy and stability, either alone or in combination with existing stabilization strategies. Despite their great potential, it is crucial to evaluate these systems in *in vivo* models or real-world conditions to further establish their use as effective countermeasures.

While there have been some significant efforts toward this goal, commercialization of these enzymes is still uncertain. High costs, manufacturing challenges, and reduced enzyme recovery pose significant barriers to the commercialization process. In order to make cost-effective, commercially viable enzymes for therapeutic use or environmental decontamination, it is essential to continuously improve these systems that can enhance enzyme productivity, activity, reusability, and storability.

Acknowledgments

The work was supported by the CounterACT Program of the National Institute of Health under Award Number R21-NS10383-01 and the National Science Foundation under Award Number IIP-1918981.

Authors contributions

Both P.K. and S.C. researched the data for the article and contributed equally to writing the article. P.K., S.C., and J.K.M. all provided substantial contributions to discussions of the content and reviewed/edited the manuscript before submission.

Competing interests

The authors declare no competing interests.

References

1. Levin, H.S. & R.L. Rodmitzky. 1976. Behavioral effects of organophosphates in man. *Clin. Toxicol.* **9:** 391–403.
2. Thakur, M., I.L. Medintz & S.A. Walper. 2019. Enzymatic bioremediation of organophosphate compounds—progress and remaining challenges. *Front. Bioeng. Biotechnol.* **7:** 289.
3. Bigley, A.N. & F.M. Raushel. 2019. The evolution of phosphotriesterase for decontamination and detoxification of organophosphorus chemical warfare agents. *Chem. Biol. Interact.* **308:** 80–88.
4. Schofield, D.A. & A.A. Dinovo. 2010. Generation of a mutagenized organophosphorus hydrolase for the biodegradation of the organophosphate pesticides malathion and demeton-S. *J. Appl. Microbiol.* **109:** 548–557.
5. Leikin, J.B., R.G. Thomas, F.G. Walter, *et al*. 2002. A review of nerve agent exposure for the critical care physician. *Crit. Care Med.* **30:** 2346–2354.
6. Raushel, F.M. 2002. Bacterial detoxification of organophosphate nerve agents. *Curr. Opin. Microbiol.* **5:** 288–295.
7. Marrs, T.C. 1993. Organophosphate poisoning. *Pharmacol. Ther.* **58:** 51–66.
8. Gunnell, D., M. Eddleston, M.R. Phillips, *et al*. 2007. The global distribution of fatal pesticide self-poisoning: systematic review. *BMC Public Health* **7**. https://doi.org/10.1186/1471-2458-7-357.
9. Mew, E.J., P. Padmanathan, F. Konradsen, *et al*. 2017. The global burden of fatal self-poisoning with pesticides 2006–15: systematic review. *J. Affect. Disord.* **219:** 93–104.
10. Bird, S.B., R.J. Gaspari & E.W. Dickson. 2003. Early death due to severe organophosphate poisoning is a centrally mediated process. *Acad. Emerg. Med.* **10:** 295–298.
11. Kok, A. 1993. REM sleep pathways and anticholinesterase intoxication: a mechanism for nerve agent-induced, central respiratory failure. *Med. Hypotheses* **41:** 141–149.

12. Goswamy, R., A. Chaudhuri & A. Mahashur. 1994. Study of respiratory failure in organophosphate and carbamate poisoning. *Heart Lung* **23:** 466–472.
13. Tafuri, J. & J. Roberts. 1987. Organophosphate poisoning. *Ann. Emerg. Med.* **16:** 193–202.
14. Eddleston, M., N.A. Buckley, P. Eyer, *et al*. 2008. Management of acute organophosphorus pesticide poisoning. *Lancet* **371:** 597–607.
15. Weissman, B.A. & L. Raveh. 2008. Therapy against organophosphate poisoning: the importance of anticholinergic drugs with antiglutamatergic properties. *Toxicol. Appl. Pharmacol.* **232:** 351–358.
16. Schultz, M.K., L.K. Wright, M.F. Stone, *et al*. 2012. The anticholinergic and antiglutamatergic drug caramiphen reduces seizure duration in soman-exposed rats: synergism with the benzodiazepine diazepam. *Toxicol. Appl. Pharmacol.* **259:** 376–386.
17. Schultz, M.K., L.K. Wright, M. de Araujo Furtado, *et al*. 2014. Caramiphen edisylate as adjunct to standard therapy attenuates soman-induced seizures and cognitive deficits in rats. *Neurotoxicol. Teratol.* **44:** 89–104.
18. Figueiredo, T.H., V. Aroniadou-Anderjaska, F. Qashu, *et al*. 2011. Neuroprotective efficacy of caramiphen against soman and mechanisms of its action. *Br. J. Pharmacol.* **164:** 1495–1505.
19. Worek, F., H. Thiermann & T. Wille. 2016. Oximes in organophosphate poisoning: 60 years of hope and despair. *Chem. Biol. Interact.* **259**(Part B)**:** 93–98.
20. Pang, Z., C.-M.J. Hu, R.H. Fang, *et al*. 2015. Detoxification of organophosphate poisoning using nanoparticle bioscavengers. *ACS Nano* **9:** 6450–6458.
21. Masson, P. 2015. Chapter 75 — Catalytic bioscavengers: the new generation of bioscavenger-based medical countermeasures. In *Handbook of Toxicology of Chemical Warfare Agents*. 2nd ed. R.C. Gupta, Ed.: 1107–1123. Boston, MA: Academic Press.
22. Lenz, D.E., D. Yeung, J.R. Smith, *et al*. 2007. Stoichiometric and catalytic scavengers as protection against nerve agent toxicity: a mini review. *Toxicology* **333:** 31–39.
23. Jackson, C.J., A. Carville, J. Ward, *et al*. 2014. Use of OpdA, an organophosphorus (OP) hydrolase, prevents lethality in an African green monkey model of acute OP poisoning. *Toxicology* **317:** 1–5.
24. Munnecke, D.M. & D.P. Hsieh. 1974. Microbial decontamination of parathion and p-nitrophenol in aqueous media. *Appl. Microbiol.* **28:** 212–217.
25. Dumas, D.P., S.R. Caldwell, J.R. Wild, *et al*. 1989. Purification and properties of the phosphotriesterase from *Pseudomonas diminuta*. *J. Biol. Chem.* **264:** 19659–19665.
26. Goldsmith, M. & Y. Ashani. 2018. Catalytic bioscavengers as countermeasures against organophosphate nerve agents. *Chem. Biol. Interact.* **292:** 50–64.
27. Watkins, L.M., H.J. Mahoney, J.K. McCulloch, *et al*. 1997. Augmented hydrolysis of diisopropyl fluorophosphate in engineered mutants of phosphotriesterase. *J. Biol. Chem.* **272:** 25596–25601.
28. Caldwell, S.R., J.R. Newcomb, K.A. Schlecht, *et al*. 1991. Limits of diffusion in the hydrolysis of substrates by the phosphotriesterase from *Pseudomonas diminuta*. *Biochemistry* **30:** 7438–7444.
29. Farnoosh, G. & A.M. Latifi. 2014. A review on engineering of organophosphorus hydrolase (OPH) enzyme. *J. Appl. Biotechnol. Rep.* **1:** 1–10.
30. Reeves, T.E., M.E. Wales, J.K. Grimsley, *et al*. 2008. Balancing the stability and the catalytic specificities of OP hydrolases with enhanced V-agent activities. *Protein Eng. Des. Sel.* **21:** 405–412.
31. Omburo, G.A., J.M. Kuo, L.S. Mullins, *et al*. 1992. Characterization of the zinc binding site of bacterial phosphotriesterase. *J. Biol. Chem.* **267:** 13278–13283.
32. Bigley, A.N. & F.M. Raushel. 2013. Catalytic mechanisms for phosphotriesterases. *Biochim. Biophys. Acta* **1834:** 443–453.
33. Goldsmith, M., N. Aggarwal, Y. Ashani, *et al*. 2017. Overcoming an optimization plateau in the directed evolution of highly efficient nerve agent bioscavengers. *Protein Eng. Des. Sel.* **30:** 333–345.
34. Benning, M.M., J.M. Kuo, F.M. Raushel, *et al*. 1994. Three-dimensional structure of phosphotriesterase: an enzyme capable of detoxifying organophosphate nerve agents. *Biochemistry* **33:** 15001–15007.
35. Chen-Goodspeed, M., M.A. Sogorb, F. Wu, *et al*. 2001. Enhancement, relaxation, and reversal of the stereoselectivity for phosphotriesterase by rational evolution of active site residues. *Biochemistry* **40:** 1332–1339.
36. Tsai, P.-C., A. Bigley, Y. Li, *et al*. 2010. Stereoselective hydrolysis of organophosphate nerve agents by the bacterial phosphotriesterase. *Biochemistry* **49:** 7978–7987.
37. diSioudi, B., J.K. Grimsley, K. Lai, *et al*. 1999. Modification of near active site residues in organophosphorus hydrolase reduces metal stoichiometry and alters substrate specificity. *Biochemistry* **38:** 2866–2872.
38. Bigley, A.N., C. Xu, T.J. Henderson, *et al*. 2013. Enzymatic neutralization of the chemical warfare agent VX: evolution of phosphotriesterase for phosphorothiolate hydrolysis. *J. Am. Chem. Soc.* **135:** 10426–10432.
39. Tsai, P.C., N. Fox, A.N. Bigley, *et al*. 2012. Enzymes for the homeland defense: optimizing phosphotriesterase for the hydrolysis of organophosphate nerve agents. *Biochemistry* **51:** 6463–6475.
40. Bigley, A.N., E. Desormeaux, D.F. Xiang, *et al*. 2019. Overcoming the challenges of enzyme evolution to adapt phosphotriesterase for V-agent decontamination. *Biochemistry* **58:** 2039–2053.
41. Grimsley, J.K., B. Calamini, J.R. Wild, *et al*. 2005. Structural and mutational studies of organophosphorus hydrolase reveal a cryptic and functional allosteric-binding site. *Arch. Biochem. Biophys.* **442:** 169–179.
42. Carletti, E., L. Jacquamet, M. Loiodice, *et al*. 2009. Update on biochemical properties of recombinant *Pseudomonas diminuta* phosphotriesterase. *J. Enzyme Inhib. Med. Chem.* **24:** 1045–1055.
43. Mee-Hie Cho, C.M.-H., A. Mulchandani & W. Chen. 2006. Functional analysis of organophosphorus hydrolase variants with high degradation activity towards organophosphate pesticides. *Protein Eng. Des. Sel.* **19:** 99–105.

44. Cho, C.M.-H., A. Mulchandani & W. Chen. 2004. Altering the substrate specificity of organophosphorus hydrolase for enhanced hydrolysis of chlorpyrifos. *Appl. Environ. Microbiol.* **70:** 4681–4685.
45. Olsen, A.J., L.A. Halvorsen, C.Y. Yang, *et al*. 2017. Impact of phenylalanines outside the dimer interface on phosphotriesterase stability and function. *Mol. Biosyst*. **13:** 2092–2106.
46. Jeong, Y.S., J.M. Choi, H.H. Kyeong, *et al*. 2014. Rational design of organophosphorus hydrolase with high catalytic efficiency for detoxifying a V-type nerve agent. *Biochem. Biophys. Res. Commun.* **449:** 263–267.
47. Farnoosh, G., K. Khajeh, A.M. Latifi, *et al*. 2016. Engineering and introduction of *de novo* disulphide bridges in organophosphorus hydrolase enzyme for thermostability improvement. *J. Biosci.* **41:** 577–588.
48. Baker, P.J. & J.K. Montclare. 2011. Enhanced refoldability and thermoactivity of fluorinated phosphotriesterase. *ChemBioChem* **12:** 1845–1848.
49. Yang, C.Y., P.D. Renfrew, A.J. Olsen, *et al*. 2014. Improved stability and half-life of fluorinated phosphotriesterase using Rosetta. *ChemBioChem* **15:** 1761–1764.
50. Jacob, R.B., F. Ding, D. Ye, *et al*. 2015. Computational redesign reveals allosteric mutation hotspots of organophosphate hydrolase that enhance organophosphate hydrolysis. United States. https://www.osti.gov/servlets/purl/1427256.
51. Cherny, I., P. Greisen, Jr., Y. Ashani, *et al*. 2013. Engineering V-type nerve agents detoxifying enzymes using computationally focused libraries. *ACS Chem. Biol.* **8:** 2394–2403.
52. Bigley, A.N., M.F. Mabanglo, S.P. Harvey, *et al*. 2015. Variants of phosphotriesterase for the enhanced detoxification of the chemical warfare agent VR. *Biochemistry* **54:** 5502–5512.
53. Khersonsky, O., R. Lipsh, Z. Avizemer, *et al*. 2018. Automated design of efficient and functionally diverse enzyme repertoires. *Mol. Cell* **72:** 178–186.e175.
54. Grahame, D.A.S., B.C. Bryksa & R.Y. Yada. 2015. Factors affecting enzyme activity. In *Improving and Tailoring Enzymes for Food Quality and Functionality*. R.Y. Yada, Ed.: 11–55. Cambridge: Woodhead Publishing.
55. Ohtake, S., Y. Kita & T. Arakawa. 2011. Interactions of formulation excipients with proteins in solution and in the dried state. *Adv. Drug Deliv. Rev.* **63:** 1053–1073.
56. Satvik Iyengar, A.R., R.K. Tripathy, P. Bajaj, *et al*. 2015. Improving storage stability of recombinant organophosphorus hydrolase. *Protein Expr. Purif.* **111:** 28–35.
57. Yang, J.S. & L. Yang. 2013. Preparation and application of cyclodextrin immobilized polysaccharides. *J. Mater. Chem. B* **1:** 909–918.
58. Desire, B. & S. Saint-Andre. 1986. Interaction of soman with β-cyclodextrin. *Fundam. Appl. Toxicol.* **7:** 646–657.
59. Moon, Y., A.T. Jafry, S. Bang Kang, *et al*. 2019. Organophosphorus hydrolase-poly-beta-cyclodextrin as a stable self-decontaminating bio-catalytic material for sorption and degradation of organophosphate pesticide. *J. Hazard. Mater.* **365:** 261–269.
60. Veronese, F.M. 2001. Peptide and protein PEGylation: a review of problems and solutions. *Biomaterials* **22:** 405–417.
61. Novikov, B.N., J.K. Grimsley, R.J. Kern, *et al*. 2010. Improved pharmacokinetics and immunogenicity profile of organophosphorus hydrolase by chemical modification with polyethylene glycol. *J. Control. Release* **146:** 318–325.
62. Andreopoulos, F.M., M.J. Roberts, M.D. Bentley, *et al*. 1999. Photoimmobilization of organophosphorus hydrolase within a PEG-based hydrogel. *Biotechnol. Bioeng.* **65:** 579–588.
63. Zhang, P., E.J. Liu, C. Tsao, *et al*. 2019. Nanoscavenger provides long-term prophylactic protection against nerve agents in rodents. *Sci. Transl. Med.* **11:** eaau7091.
64. Kim, M., M. Gkikas, A. Huang, *et al*. 2014. Enhanced activity and stability of organophosphorus hydrolase via interaction with an amphiphilic polymer. *Chem. Commun. (Camb.)* **50:** 5345–5348.
65. Cheng, H., Y. Zhao, X. Luo, *et al*. 2018. Cross-linked enzyme–polymer conjugates with excellent stability and detergent-enhanced activity for efficient organophosphate degradation. *Bioresour. Bioprocess.* **5:** 49.
66. Suthiwangcharoen, N. & R. Nagarajan. 2014. Enhancing enzyme stability by construction of polymer–enzyme conjugate micelles for decontamination of organophosphate agents. *Biomacromolecules* **15:** 1142–1152.
67. Komives, C.F., E. Lilley & A.J. Russell. 1994. Biodegradation of pesticides in nonionic water-in-oil microemulsions of tween 85: relationship between micelle structure and activity. *Biotechnol. Bioeng.* **43:** 946–959.
68. Mills, C.E., A. Obermeyer, X. Dong, *et al*. 2016. Complex coacervate core micelles for the dispersion and stabilization of organophosphate hydrolase in organic solvents. *Langmuir* **32:** 13367–13376.
69. Lee, Y., I. Stanish, V. Rastogi, *et al*. 2003. Sustained enzyme activity of organophosphorus hydrolase in polymer encased multilayer assemblies. *Langmuir* **19:** 1330–1336.
70. Singh, A., Y. Lee & W.J. Dressick. 2004. Self-cleaning fabrics for decontamination of organophosphorous pesticides and related chemical agents. *Adv. Mater.* **16:** 2112–2115.
71. Panganiban, B., B. Qiao, T. Jiang, *et al*. 2018. Random heteropolymers preserve protein function in foreign environments. *Science* **359:** 1239–1243.
72. Havens, P.L. & H.F. Rase. 1993. Reusable immobilized enzyme/polyurethane sponge for removal and detoxification of localized organophosphate pesticide spills. *Ind. Eng. Chem. Res.* **32:** 2254–2258.
73. Lejeune, K.E. & A.J. Russell. 1996. Covalent binding of a nerve agent hydrolyzing enzyme within polyurethane foams. *Biotechnol. Bioeng.* **51:** 450–457.
74. LeJeune, K.E., A.J. Mesiano, S.B. Bower, *et al*. 1997. Dramatically stabilized phosphotriesterase-polymers for nerve agent degradation. *Biotechnol. Bioeng.* **54:** 105–114.
75. LeJeune, K.E., J.R. Wild & A.J. Russell. 1998. Nerve agents degraded by enzymatic foams. *Nature* **395:** 27–28.
76. Kluge, J.A., A.B. Li, B.T. Kahn, *et al*. 2016. Silk-based blood stabilization for diagnostics. *Proc. Natl. Acad. Sci. USA* **113:** 5892–5897.
77. Dennis, P.B., A.Y. Walker, M.B. Dickerson, *et al*. 2012. Stabilization of organophosphorus hydrolase by entrapment in silk fibroin: formation of a robust enzymatic material

suitable for surface coatings. *Biomacromolecules* **13:** 2037–2045.
78. Raynes, J.K., F.G. Pearce, S.J. Meade, *et al*. 2011. Immobilization of organophosphate hydrolase on an amyloid fibril nanoscaffold: towards bioremediation and chemical detoxification. *Biotechnol. Prog.* **27:** 360–367.
79. Kanugula, A.K., E.R. Repalle, J.P. Pandey, *et al.* 2011. Immobilization of organophosphate hydrolase on biocompatible gelatin pads and its use in removal of organophosphate compounds and nerve agents. *Indian J. Biochem. Biophys.* **48:** 29–34.
80. Pei, L., G. Omburo, W.D. McGuinn, *et al.* 1994. Encapsulation of phosphotriesterase within murine erythrocytes. *Toxicol. Appl. Pharmacol.* **124:** 296–301.
81. Budai, M., P. Chapela, P. Grof, *et al*. 2009. Physicochemical characterization of stealth liposomes encapsulating an organophosphate hydrolyzing enzyme. *J. Liposome Res.* **19:** 163–168.
82. Petrikovics, I., K. Hong, G. Omburo, *et al*. 1999. Antagonism of paraoxon intoxication by recombinant phosphotriesterase encapsulated within sterically stabilized liposomes. *Toxicol. Appl. Pharmacol.* **156:** 56–63.
83. Lawson, G.E., Y. Lee, F.M. Raushel, *et al*. 2005. Phospholipid-based catalytic nanocapsules. *Adv. Funct. Mater.* **15:** 267–272.
84. Lawson, G.E., Y. Lee & A. Singh. 2003. Formation of stable nanocapsules from polymerizable phospholipids. *Langmuir* **19:** 6401–6407.
85. Xu, J., J. Sun, Y. Wang, *et al*. 2014. Application of iron magnetic nanoparticles in protein immobilization. *Molecules* **19:** 11465–11486.
86. Robatjazi, S.R., M. Reihani, S. Mahboudi, *et al.* 2017. Immobiliztion of organophosphorus hydrolase enzyme on ferric magnetic nanoparticles and investigation of immobilized enzyme stability. *J. Microbiol. Biotechnol. Food Sci.* **6:** 1295–1299.
87. Chen, Y., Z. Luo & X. Lu. 2019. Construction of novel enzyme–graphene oxide catalytic interface with improved enzymatic performance and its assembly mechanism. *ACS Appl. Mater. Interfaces* **11:** 11349–11359.
88. Lei, C., Y. Shin, J. Liu, *et al.* 2002. Entrapping enzyme in a functionalized nanoporous support. *J. Am. Chem. Soc.* **124:** 11242–11243.
89. Frančič, N., A. Košak & A. Lobnik. 2016. Immobilisation of organophosphate hydrolase on mesoporous and Stöber particles. *J. Sol-Gel Sci. Technol.* **79:** 497–509.
90. Caldwell, S.R. & F.M. Raushel. 1991. Detoxification of organophosphate pesticides using an immobilized phosphotriesterase from *Pseudomonas diminuta*. *Biotechnol. Bioeng.* **37:** 103–109.
91. Sharifi, M., S. Robatjazi, M. Sadri, *et al*. 2018. Covalent immobilization of organophosphorus hydrolase enzyme on chemically modified cellulose microfibers: statistical optimization and characterization. *React. Funct. Polym.* **124:** 162–170.
92. Milani, M.M., A.S. Lotfi, A. Mohsenifar, *et al.* 2015. Enhancing organophosphorus hydrolase stability by immobilization on chitosan beads containing glutaraldehyde. *Res. J. Environ. Toxicol.* **9:** 34–44.
93. Ji, X., J. Zheng, J. Xu, *et al*. 2005. (CdSe)ZnS quantum dots and organophosphorus hydrolase bioconjugate as biosensors for detection of paraoxon. *J. Phys. Chem. B* **109:** 3793–3799.
94. Pedrosa, V.A., S. Paliwal, S. Balasubramanian, *et al*. 2010. Enhanced stability of enzyme organophosphate hydrolase interfaced on the carbon nanotubes. *Colloids Surf. B Biointerfaces* **77:** 69–74.
95. Karami, R., A. Mohsenifar, S.M. Mesbah Namini, *et al*. 2016. A novel nanobiosensor for the detection of paraoxon using chitosan-embedded organophosphorus hydrolase immobilized on Au nanoparticles. *Prep. Biochem. Biotechnol.* **46:** 559–566.
96. Xiong, S., Y. Deng, Y. Zhou, *et al*. 2018. Current progress in biosensors for organophosphorus pesticides based on enzyme functionalized nanostructures: a review. *Anal. Methods* **10:** 5468–5479.
97. Breger, J.C., S. Buckhout-White, S.A. Walper, *et al*. 2017. Assembling high activity phosphotriesterase composites using hybrid nanoparticle peptide-DNA scaffolded architectures. *Nano Futures* **1:** 011002.
98. Alves, N.J., K.B. Turner, I.L. Medintz, *et al*. 2016. Protecting enzymatic function through directed packaging into bacterial outer membrane vesicles. *Sci. Rep.* **6:** 24866.
99. Raveh, L., Y. Segall, H. Leader, *et al*. 1992. Protection against tabun toxicity in mice by prophylaxis with an enzyme hydrolyzing organophosphate esters. *Biochem. Pharmacol.* **44:** 397–400.
100. Misik, J., R. Pavlikova, J. Cabal, *et al*. 2015. Acute toxicity of some nerve agents and pesticides in rats. *Drug Chem. Toxicol.* **38:** 32–36.
101. Shaffer, C.B. & B. West. 1960. The acute and subacute toxicity of technical O,O-diethyl S-2-diethylaminoethyl phosphorothioate hydrogen oxalate (Tetram). *Toxicol. Appl. Pharmacol.* **2:** 1–13.
102. Rice, H., C.H. Dalton, M.E. Price, *et al*. 2015. Toxicity and medical countermeasure studies on the organophosphorus nerve agents VM and VX. *Proc. Math. Phys. Eng. Sci*. **471:** 20140891.
103. Houze, P., T. Berthin, J.H. Raphalen, *et al*. 2018. High dose of pralidoxime reverses paraoxon-induced respiratory toxicity in mice. *Turk. J. Anaesthesiol. Reanim.* **46:** 131–138.
104. Moore, P.G. & O.F. James. 1981. Acute pancreatitis induced by acute organophosphate poisoning. *Postgrad. Med. J.* **57:** 660–662.
105. Rattner, B.A. & D.J. Hoffman. 1984. Comparative toxicity of acephate in laboratory mice, white-footed mice, and meadow voles. *Arch. Environ. Contam. Toxicol.* **13:** 483–491.
106. Roodveldt, C. & D.S. Tawfik. 2005. Directed evolution of phosphotriesterase from *Pseudomonas diminuta* for heterologous expression in *Escherichia coli* results in stabilization of the metal-free state. *Protein Eng. Des. Sel.* **18:** 51–58.
107. Benning, M.M., H. Shim, F.M. Raushel, *et al*. 2001. High resolution X-ray structures of different metal-substituted forms of phosphotriesterase from *Pseudomonas diminuta*. *Biochemistry* **40:** 2712–2722.